



## On the size distribution of Atlantic tropical cyclones

L. Dean,<sup>1</sup> K. A. Emanuel,<sup>2</sup> and D. R. Chavas<sup>2</sup>

Received 12 May 2009; revised 10 June 2009; accepted 15 June 2009; published 17 July 2009.

[1] The size of a tropical cyclone is known to vary considerably across storms, though little is understood about the environmental and internal factors that modulate it. Making use of newly available extended tropical cyclone records that include information about storm structure, we examine the size distribution of Atlantic tropical cyclones, using as a metric the radius of vanishing storm winds normalized by the theoretical upper bound given by the ratio of the potential intensity to the Coriolis parameter. We find that the distribution of this normalized outer radius is closely log-normal. **Citation:** Dean, L., K. A. Emanuel, and D. R. Chavas (2009), On the size distribution of Atlantic tropical cyclones, *Geophys. Res. Lett.*, *36*, L14803, doi:10.1029/2009GL039051.

### 1. Introduction

[2] Despite recognition of the wide range of observed sizes of tropical cyclones, the underlying internal and environmental factors that determine both individual storm size and the climatological size distribution remain enigmatic. In the absence of land interaction, the size of a storm is observed in nature to vary only marginally during its lifetime prior to recurvature into the extra-tropics; however, significant variation exists between storms, regardless of basin, location, and time of year [Merrill, 1984]. For example, the radius of tropical storm force winds ( $>17.5 \text{ ms}^{-1}$ ) was 2200 km in super typhoon Tip (1974, West Pacific), whereas this radius was a mere 48 km in Cyclone Tracy (1974, Australia).

[3] Theoretical approaches may provide useful insight. Emanuel [1986] represented a tropical cyclone as a vortex characterized by approximately constant saturation potential vorticity and nearly constant boundary layer relative humidity outside the core, which leads to a direct relationship between inner core structure, maximum wind speed, Coriolis parameter  $f$ , and outer storm radius. Indeed, such general relationships have been observed in nature [Weatherford and Gray, 1988]. One consequence of this theory is the requirement that the circulation of a tropical cyclone vanish at a finite radius whose upper bound scales as  $\frac{V_{pot}}{f}$  (typical values are 1000 km), where  $V_{pot}$  is the maximum attainable wind speed [Emanuel, 1986]; no known theoretical lower bound currently exists. Numerical modeling approaches [e.g., Rotunno and Emanuel, 1987; Emanuel, 1989] suggest

that tropical cyclone maximum wind speed and evolution are relatively insensitive to storm size except as the outer radius approaches the upper bound given by  $\frac{V_{pot}}{f}$ .

[4] Observational investigation of tropical cyclone size has often been hampered by the lack of size information in standard tropical cyclone data sets. Recently, though, two new data sets have been created that record various metrics of storm structure for Atlantic tropical cyclones: Demuth *et al.* [2006] and Kossin *et al.* [2007], both of which report several identical metrics of storm structure, including radii of maximum wind, 64-kt wind, 50-kt wind, and 34-kt wind, and in the case of Demuth *et al.* [2006], radius of outermost closed surface isobar (ROCI). However, Frank [1977] noted that while the inner core intensity of a given storm may fluctuate substantially, the broad outer circulation tends to conform to a single constant scale during its lifetime, although this scale may itself vary substantially across storms.

[5] Thus, based on the work of Frank [1977], we proceed to characterize the climatological size distribution of Atlantic tropical cyclones under the hypothesis that the outer radius of the storm, defined here as the radius at which perturbations in the surface wind directly associated with the storm vanish, is the least variable among the various size metrics over the lifetime of individual storms and thus is the most amenable for size distribution analysis. Because this exact metric is not included in the available data sets, and given that the ROCI differs from the true outer radius according to the pressure increment used in surface analyses and the ambient distribution of surface pressure, we elect to use a wind model based on the radius of 34-kt winds to estimate outer storm radius and its climatological distribution.

### 2. Data

[6] This work combines two data sets which report metrics of Atlantic tropical cyclone structure. First, Demuth *et al.* [2006], which spans the period 1988–2006 and includes 4669 storm fixes over water, is based on observations from aircraft, surface reports (e.g. ships), and satellite imagery and includes estimates of the radii of maximum wind, 64 kt wind, 50 kt wind, and 34-kt wind, as well as the radius of the outermost closed surface isobar (ROCI). These data are taken from National Hurricane Center (NHC) operational estimates through 2003 and from post-analyzed NHC estimates thereafter with the exception of ROCI, which is not reanalyzed. Second, Kossin *et al.* [2007], which spans the period 1983–2005 and includes 12162 storm fixes over water, is based primarily on satellite-based infrared measurements and includes identical metrics with the exception of ROCI. However, given that the satellite algorithm was trained on the Demuth *et al.* [2006] data over

<sup>1</sup>Biomedical Engineering, Johns Hopkins University, Baltimore, Maryland, USA.

<sup>2</sup>Department of Earth, Atmosphere, and Planetary Sciences, Massachusetts Institute of Technology, Cambridge, Massachusetts, USA.

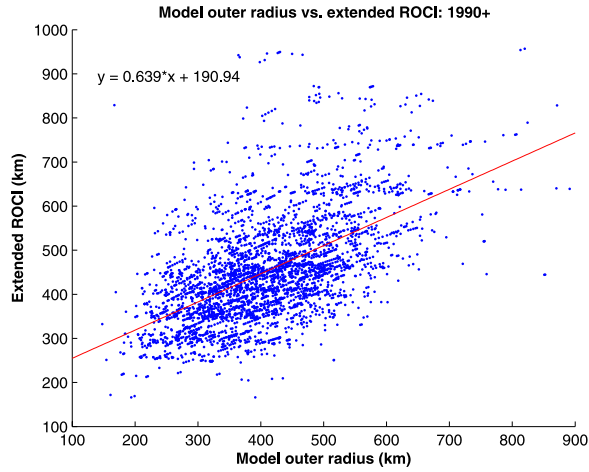


**Figure 1.** Model radius (km) versus Extended ROCI (km) taken from the *Demuth et al.* [2006] data set. Only storm fixes since 1990 are included.

the period 1995–2004, the latter data set is not truly independent.

[7] For the subset of 4,483 overlapping samples (i.e. same storm and time recorded in both data sets) the radius of 34-kt winds was compared. While there exists significant spread ( $r^2 = .302$ ), the regression slope of 0.98 between the two data sets is reassuringly close to unity.

### 3. Estimating Outer Radius $r_0$

#### 3.1. Methodology

[8] Given that *Kossin et al.* [2007] does not contain a metric for outer storm radius,  $r_0$ , and that ROCI is not a consistent measure of  $r_0$ , we elect instead to derive  $r_0$  from the radius of 34-kt winds,  $r_{34}$ , together with a theoretical outer wind structure model, which is described in detail by *Emanuel* [2004] and is reviewed here. The flow is assumed to be steady and axisymmetric. Outside of  $r_{34}$  the model assumes little if any deep convection, resulting in a local balance between subsidence warming and radiative cooling. Furthermore, given that both the lapse rate and the rate of clear-sky radiative cooling are nearly constant in the tropics, the equilibrium subsidence velocity,  $w_{rad}$ , can be taken to be approximately constant. In equilibrium, this subsidence rate must match the rate of Ekman suction-induced entrainment of free tropospheric air into the boundary layer in order to prevent the creation of large vertical temperature gradients across the top of the boundary layer.

[9] The angular momentum balance of the subcloud layer, assuming that it is nearly steady, is given by

$$-\frac{1}{r} \frac{\partial \psi}{\partial z} \frac{\partial M}{\partial r} = -r \frac{\partial \tau_\theta}{\partial z} \quad (1)$$

where  $\psi$  is the mass streamfunction,  $\tau_\theta$  is the azimuthal turbulent stress, and  $M$  is the absolute angular momentum per unit mass, given by

$$M = rV + \frac{1}{2}fr^2 \quad (2)$$

where  $V$  is the azimuthal velocity and  $f$  the Coriolis parameter. In (1) and (2),  $r$  and  $z$  are the radial and vertical coordinates, respectively. Integrating (1) vertically through the subcloud layer, and assuming that the turbulent stress vanishes at its top while the streamfunction vanishes at the surface, gives

$$\frac{\partial(rV)}{\partial r} \approx \frac{r^2 C_D V^2}{\psi} - fr \quad (3)$$

where  $\tau_{\theta_s}$  is replaced with a standard bulk aerodynamic formulation with drag coefficient  $C_D$  and  $M$  is replaced by the expression given in (2). The assumption of constant vertical velocity at the top of the subcloud layer implies

$$\frac{1}{r} \frac{\partial \psi}{\partial r} = -w_{rad} \quad (4)$$

It is apparent from (3) that  $\psi$  must vanish at  $r = r_0$ . Thus, integrating (4) in  $r$  and applying this outer boundary condition results in a radial profile of the streamfunction given by

$$\psi = \frac{1}{2}w_{rad}(r_0^2 - r^2) \quad (5)$$

Substituting (5) into (3) gives

$$\frac{\partial(rV)}{\partial r} = \frac{2r^2 C_D V^2}{w_{rad}(r_0^2 - r^2)} - fr \quad (6)$$

To our knowledge, this nonlinear first order differential equation has no analytical solution. However, neglecting the

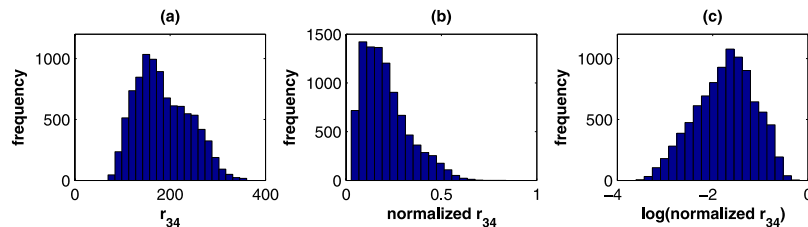


**Figure 2.** For data from *Kossin et al.* [2007], histograms of (a) the radius of 34-kt winds, (b) the radius of 34-kt winds normalized by  $\frac{V_{pot}}{f}$ , and (c) the logarithm of the data in Figure 2b.

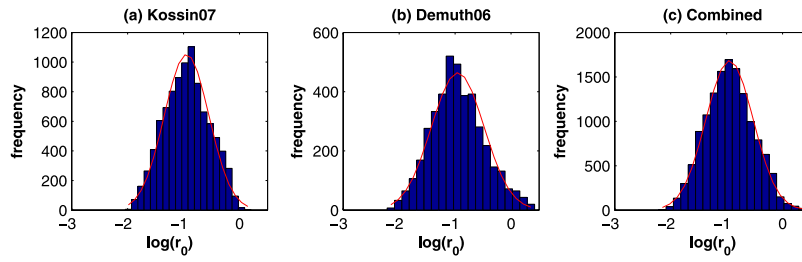


**Figure 3.** Histograms of the logarithm of the normalized outer radius for data from (a) *Kossin et al.* [2007], (b) *Demuth et al.* [2006], and (c) the combined data sets. The red curves represent a Gaussian fit to the data.

derivative on the left-hand side leads to an approximate solution given by *Emanuel* [2004]:

$$V^2 \approx \frac{f w_{rad} r_0^2 - r^2}{2C_D r} \quad (7)$$

Scale analysis of (6), with  $V$  defined according to (7) above, indicates that this approximate solution is valid except near the outer edge of the storm. The azimuthal velocity falls off as  $r^{\frac{1}{2}}$  for radii well inside  $r_0$ , but falls off more rapidly as one approaches  $r_0$ . From (7), we may deduce a specific relationship between  $r_0$  and  $r_{34}$ :

$$r_0^2 = r_{34}^2 + \frac{2C_D r_{34} V_{34}^2}{f w_{rad}} \quad (8)$$

where  $V_{34}$  is 34 knots expressed in meters per second. Finally, we use (8) to estimate  $r_0$ , taking  $C_D = 10^{-3}$  and  $w_{rad} = 1.6 \text{ cms}^{-1}$ . Our goal is to characterize the climatological distribution of outer storm radius. In principle, probability distributions should be functions of dimensionless variables, and in theory, the relevant length scale for tropical cyclones is  $\frac{V_{pot}}{f}$  [*Emanuel*, 1986]. Thus we divide  $r_0$ , as given by (8), by this length scale, taking the potential intensity from monthly mean re-analysis data [*Bister and Emanuel*, 2002] bi-linearly interpolated to the place and time of the storm observation. We include only those data from storm fixes over water and for which  $V_{pot} > 40 \text{ ms}^{-1}$  to avoid cases in which storms are rapidly transitioning to regions of cold sea surface temperatures where mature hurricanes cannot be sustained. The final data set contains 13543 fixes: 4150 from *Demuth et al.* [2006] and 9393 from *Kossin et al.* [2007].

### 3.2. Error Analysis

[10] *Demuth et al.* [2006] contains a subset of 4042 storm fixes with reported ROCI values, which can be used for model validation; *Kossin et al.* [2007] does not contain ROCI data. However, due to the fixed pressure increment applied in analysis, ROCI values will underestimate the outer radius by an amount proportional to the pressure increment, and such an error can be substantial at the periphery of a tropical cyclone due to the “flat” radial profile of pressure for large radii. Thus, we combine the wind-

radius relationship given in (7) with an assumption of gradient wind balance

$$\frac{V^2}{r} + fV = \frac{1}{\rho_0} \frac{\partial P}{\partial r} \quad (9)$$

to obtain an equation for the local pressure gradient as a function of radius,

$$\frac{\partial P}{\partial r} = \frac{f w_{rad} r_0^2 - r^2}{2C_D r^2} + f \sqrt{\frac{f w_{rad} r_0^2 - r^2}{2C_D r}} \quad (10)$$

where  $\rho_0 = 1 \text{ kgm}^{-3}$ .

[11] For the ROCI data contained by *Demuth et al.* [2006], a 1 hPa pressure increment has been employed operationally since 1990; prior to 1990, a 4 hPa increment was used but such data is less reliable due to less rigorous reporting standards. We therefore choose to exclude data prior to 1990, resulting in a final subset of 3725 storm fixes. For each remaining ROCI value, (10) is integrated iteratively to determine the radial distance corresponding to a .5 hPa extension of the pressure of outermost closed isobar reported in the data set, under the assumption that pressure increment errors are distributed uniformly (equal probability of, e.g., the true ROCI of 1013.2 hPa and 1013.7 hPa for a reported value of 1013 hPa). This “extended ROCI” data set (hereafter “ROCI-e”) provides the best available estimate of outer storm radius with which to compare model output.

[12] Figure 1 compares modeled outer radii to ROCI-e values. Model values correlate positively with reported ROCI values, albeit with a linear-fit slope of .64. The mean ROCI-e value is 8% greater than the model mean (ROCI-e: 454 km; model: 418 km). The mean absolute error (MAE) is 83.6 km, or 18% of the ROCI-e mean, which indicates significant spread between modeled and analyzed values on a case-by-case basis; errors are distributed normally (not shown).

**Table 1.** Reduced Chi-Square Goodness of Fit Values

Probability Distribution	Reduced Chi-Square Value
Log-normal	8.2
Normal	280.1
Weibull	125.5
Rayleigh	83.2
Gamma	35.5

**Table 2.** Observed Versus Expected (Gaussian) Frequencies by Bin, Log of Outer Radius

Bin	Observed Frequency	Expected Frequency	Obs-Exp
1	7	30	-23
2	39	69	-30
3	135	144	-9
4	300	274	26
5	511	474	37
6	886	741	145
7	1072	1053	19
8	1318	1358	-40
9	1562	1588	-26
10	1695	1686	9
11	1593	1624	-31
12	1311	1420	-109
13	996	1126	-130
14	791	810	-19
15	627	529	98
16	413	314	99
17	150	169	-19
18	73	82	-9
19	44	36	8
20	20	15	5

[13] Equatorward of 20°N, the model underpredicts storm size in 65% of cases with an MAE of 86 km; between 20°N and 30°N, the model underpredicts in 66% of cases with an MAE of 82 km; poleward of 30°N, the model underpredicts in 68% of cases with an MAE of 88 km. Thus, while there is a systematic model bias toward underprediction, this bias does not appear to have a significant latitudinal dependence.

#### 4. Results

[14] Figure 2a presents a histogram of the dimensional radius of 34-kt winds from *Kossin et al.* [2007]. The distribution does not obviously conform to a single common parent distribution and shows hints of bimodality. The distribution of nondimensional radius of 34-kt winds (Figure 2b) broadly resembles a log-normal distribution, including a substantial upper tail. However, Figure 2c, which gives the histogram of the logarithm of the normalized radius of 34-kt winds, illustrates the departure from log-normal, including substantial positive skew and a quasi-linear, rather than Gaussian, slope on both sides of the distribution peak.

[15] Figures 3a–3c show histograms of the logarithm of the normalized outer radius from *Kossin et al.* [2007] and *Demuth et al.* [2006], and the combined data sets (including overlapping cases), respectively; also included is a Gaussian fit to the data based on data set parameters. The distribution of the combined data sets have a mean of .424, median of .385, and standard deviation of .189. The peak of the distribution occurs near a normalized radius of approximately 0.4, corresponding to an outer radius of 400 km for typical latitude and potential intensity values.

[16] In contrast to the histograms in Figure 2, the distribution of the normalized outer radius is very nearly log-normal. A reduced chi-square metric is employed to test the goodness of fit of this distribution to the log-normal, normal, Weibull, Rayleigh, and gamma parent distributions. Table 1 displays these values.

[17] Clearly, the distribution of outer storm radius is best approximated with a log-normal parent distribution (calculated using the distribution of the logarithm of the data).

Moreover, the distribution has near-zero values for skewness (0.1) and excess kurtosis (−.3). The Kolmogorov-Smirnov test for normality, applied to the data set redimensionalized to have zero mean and unit variance, yields a p-value of .009.

[18] The full frequency distribution comparison is displayed in Table 2. The lone notable discrepancy with a potential physical explanation is the smaller observed frequencies in the lower tail compared to the expected values given by the parent distribution, which may be an indication of the existence of a lower bound on the size of tropical cyclones, although such a theoretical quantity has yet to be determined.

#### 5. Discussion and Conclusions

[19] While the inner structure of a tropical cyclone often varies significantly both during the lifetime of a storm and across storms, the outer storm radius, defined as the radius at which the perturbation winds directly associated with the storm vanish, is believed to remain relatively constant during a storm's lifetime [*Frank, 1977*]. Here we combine storm structure data from two recent Atlantic tropical cyclone data sets, together with an outer wind model, to demonstrate that the distribution of nondimensional outer storm radius, normalized by the ratio of its local maximum potential intensity to the Coriolis parameter, is closely log-normal with a median value of approximately 0.4.

[20] The log-normal nature of this distribution suggests that the size of a given tropical cyclone may be primarily a function of the geometry of the disturbance that serves to initiate it rather than a property of the large-scale environment, a theory put forward by previous studies using numerical simulation [*Rotunno and Emanuel, 1987; Emanuel, 1989*]. Whether this geometry is innate to the precursor disturbance itself prior to genesis or is determined by internal processes during genesis (or both) is not clear. Either way, the implication is that the outer radius may be viewed as the product of the ratio  $\frac{V_{pot}}{f}$  and a random draw from a log-normal probability distribution.

[21] However, we offer no definite conclusions about the physical cause of this distribution, but note with curiosity that the log-normal distribution is ubiquitous in science across a wide-range of seemingly unrelated disciplines, including the cluster aggregation of particles [*Briehl and Urbassek, 1999*], molecules and crystals [*Espiau de Lamaestre and Bernas, 2006*], total rainfall, species abundance, income, etc. [see, e.g., *Limpert et al., 2001; Mitzenmacher, 2004; Koch, 1966*]. On a practical level, a better understanding of tropical cyclone size dynamics on both a case-by-case and climatological basis would be of great value to real-time forecasting, particularly for storm surge, and to hurricane risk assessment.

[22] **Acknowledgments.** This material is based in part upon work supported by the National Science Foundation under grant ATM-0630690. Any opinions, findings, and conclusions or recommendations expressed in this material are those of the author(s) and do not necessarily reflect the views of the National Science Foundation.

#### References

Bister, M., and K. A. Emanuel (2002), Low frequency variability of tropical cyclone potential intensity: 1. Interannual to interdecadal variability, *J. Geophys. Res.*, 107(D24), 4801, doi:10.1029/2001JD000776.

- Briehl, B., and H. M. Urbassek (1999), Monte Carlo simulation of growth and decay processes in a cluster aggregation source, *J. Vac. Sci. Technol. A*, *17*, 256–265.
- Demuth, J. L., M. DeMaria, and J. A. Knaff (2006), Improvement of advanced microwave sounding unit tropical cyclone intensity and size estimation algorithms, *J. Appl. Meteorol. Climatol.*, *45*, 1573–1581.
- Emanuel, K. A. (1986), An air-sea interaction theory for tropical cyclones. Part I: Steady state maintenance, *J. Atmos. Sci.*, *42*, 1062–1071.
- Emanuel, K. A. (1989), The finite-amplitude nature of tropical cyclogenesis, *J. Atmos. Sci.*, *46*, 3431–3456.
- Emanuel, K. A. (2004), Tropical cyclone energetics and structure, in *Atmospheric Turbulence and Mesoscale Meteorology*, edited by E. Federovich, R. Rotunno, and B. Stevens, pp. 165–192, Cambridge Univ. Press, New York.
- Espiau de Lamaestre, R., and H. Bernas (2006), Significance of lognormal nanocrystal size distributions, *Phys. Rev. B*, *73*, 125317, doi:10.1103/PhysRevB.73.125317.
- Frank, W. M. (1977), Structure and energetics of the tropical cyclone: I. Storm structure, *Mon. Weather Rev.*, *105*, 1119–1135.
- Koch, A. L. (1966), The logarithm in biology. 1. Mechanisms generating the log-normal distribution exactly, *J. Theor. Biol.*, *12*, 276–290.
- Kossin, J. P., J. A. Knaff, H. I. Berger, D. C. Herndon, T. A. Cram, C. S. Velden, R. J. Murnane, and J. D. Hawkins (2007), Estimating hurricane wind structure in the absence of aircraft reconnaissance, *Weather Forecasting*, *22*, 89–101.
- Limpert, E., W. A. Stahel, and M. Abbt (2001), Log-normal distributions across the sciences: Keys and clues, *BioScience*, *51*, 341–352.
- Merrill, R. T. (1984), A comparison of large and small tropical cyclones, *Mon. Weather Rev.*, *112*, 1408–1418.
- Mitzenmacher, M. (2004), A brief history of generative models for power law and lognormal distributions, *Internet Math.*, *1*, 226–251.
- Rotunno, R., and K. A. Emanuel (1987), An air-sea interaction theory for tropical cyclones. Part II: Evolutionary study using a nonhydrostatic axisymmetric numerical model, *J. Atmos. Sci.*, *44*, 542–561.
- Weatherford, C. L., and W. M. Gray (1988), Typhoon structure as revealed by aircraft reconnaissance. Part II: Structural variability, *Mon. Weather Rev.*, *116*, 1044–1056.

---

D. R. Chavas and K. A. Emanuel, Department of Earth, Atmosphere, and Planetary Sciences, Massachusetts Institute of Technology, Cambridge, MA 02139, USA. (drchavas@gmail.com; emanuel@mit.edu)

L. Dean, Johns Hopkins University, Baltimore, MD 21218, USA. (ldean4@jhu.edu)